Supporting information:

A novel carbazole derivative containing fluorobenzene unit: Aggregation-induced fluorescence emission, polymorphism, mechanochromism and non-reversible thermo-stimulus fluorescence

Huichao Zhu[a], Shiyin Weng[a], Hong Zhang[a], Haizhu Yu[a], Lin Kong[a], Yulin Zhong*[b], Yupeng Tian[a], Jiaxiang Yang*[a]

[a]*College of Chemistry and Chemical Engineering, Anhui University, Anhui Province Key Laboratory of Chemistry for Inorganic/Organic Hybrid Functionalized Materials, Hefei 230601, P. R. China. E-mail: jxyang@ahu.edu.cn*
[b]*Centre for Clean Environment and Energy, Gold Coast Campus, Griffith University, Gold Coast, QLD 4222, Australia. E-mail: y.zhong@griffith.edu.au.*

Contents:

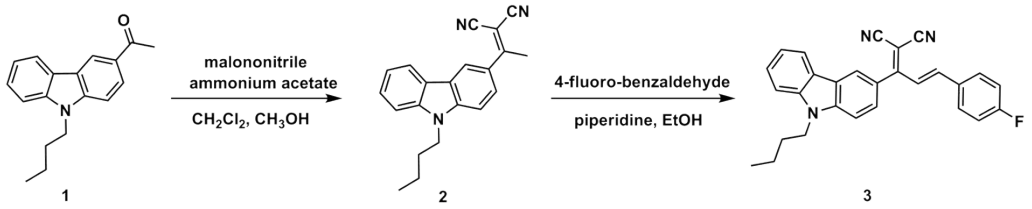

Scheme S1 Synthetic routes of compound **3**

Table S1 Crystal data and details of collection and refinement of **3Y** and **3O**.

Identification code	**3Y**	**3O**
CCDC	1511130	1576277
Empirical formula	$C_{28}H_{22}FN_3$	$C_{28}H_{22}FN_3$
Formula weight	419.49	419.48
Temperature (K)	296(2)	296(2)
Wavelength (Å)	0.71073	0.71073
Crystal system, space group	Orthorhombic, $P2_12_12_1$	Monoclinic, $P2_1/c$
a (Å)	8.7593(18)	12.758(5)
b (Å)	13.386(4)	14.223(5)
c (Å)	19.541(4)	12.808(5)
α (deg)	90	90
β (deg)	90	93.522(4)
γ (deg)	90	90
Volume (Å^3)	2291.2(9)	2319.8(14)
Z, Calculated density (Mg/m^3)	4, 1.216	4, 1.201
Absorption coefficient (mm^{-1})	0.078	0.077
F(000)	880	880
Crystal size (mm)	0.19 × 0.18 × 0.17	0.19 × 0.18 × 0.17
Theta range for data collection (deg)	1.84 to 25.00 .	1.599 to 24.999
Limiting indices	-10<=h<=10, -15<=k<=15, -21<=l<=23	-15<=h<=14, -16<=k<=16, -15<=l<=14
Reflections collected / unique	16322 / 4029	16199 / 4073
R(int)	0.0199	0.0521
Data / restraints / parameters	4029 / 0 / 291	4073 / 23 / 290
Goodness-of-fit on F^2	1.049	1.064
Final R indices [I>2sigma(I)]	R_1 = 0.0395, wR_2 = 0.1048	R_1 = 0.0879, wR_2 = 0.2700
R indices (all data)	R_1 = 0.0458, wR_2 = 0.1106	R_1 = 0.1019, wR_2 = 0.2873

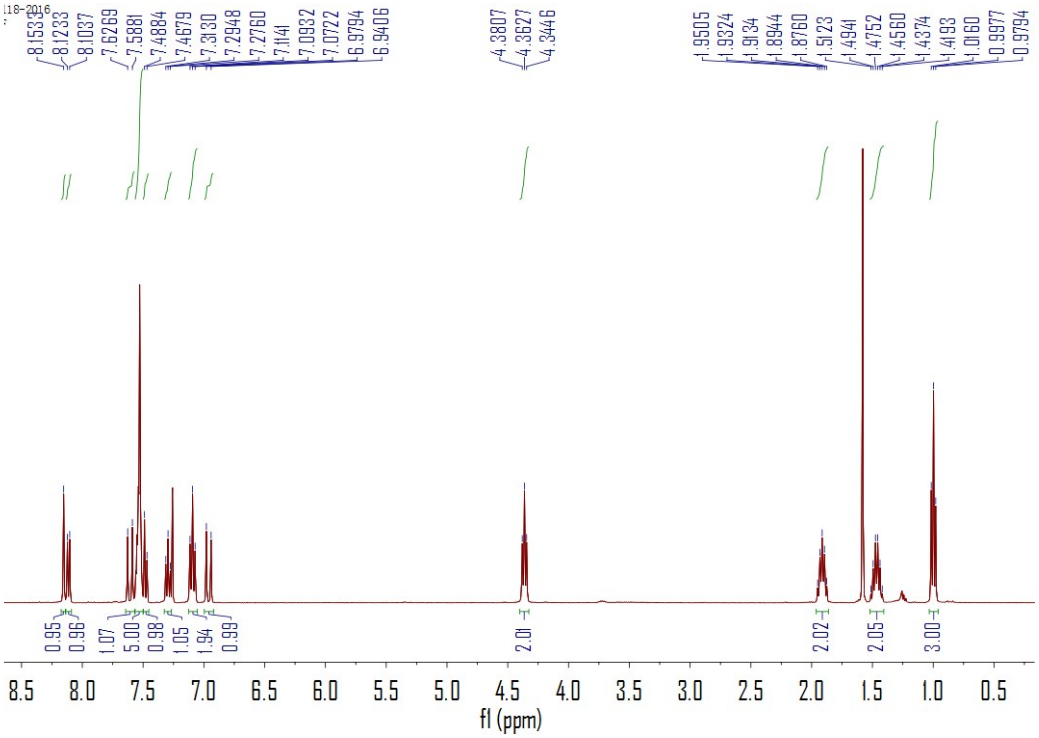

Fig. S1 ^{1}H NMR of compound **3** ($CDCl_3$, 400 MHz)

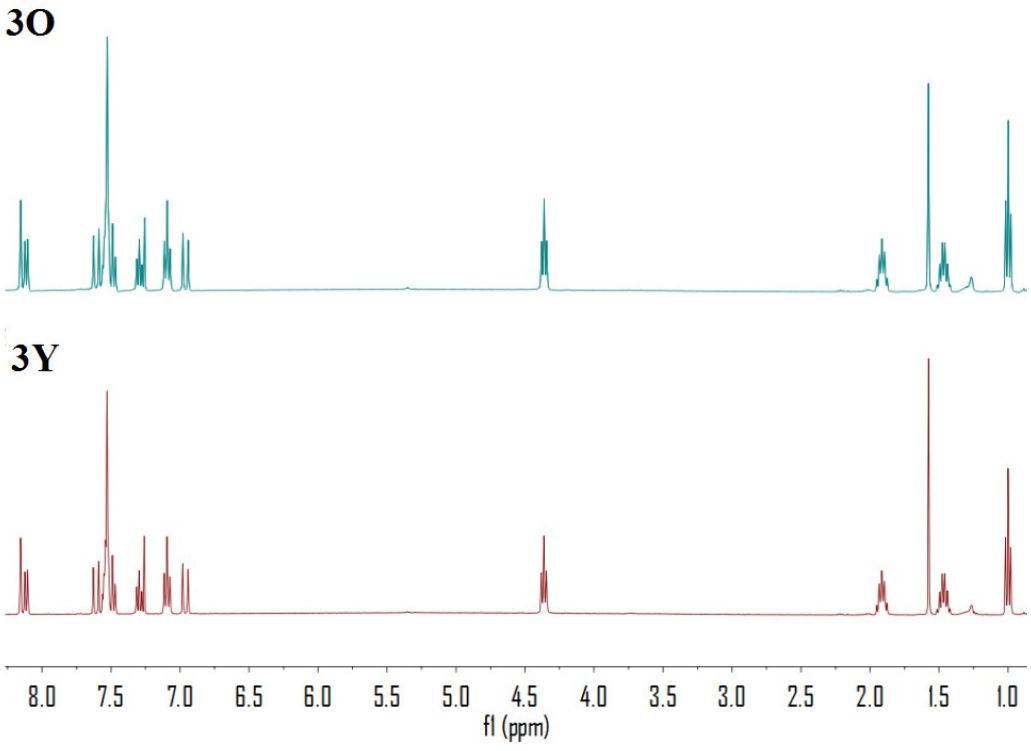

Fig. S2 ^{1}H NMR of compound **3Y** and **3O** ($CDCl_3$, 400 MHz)

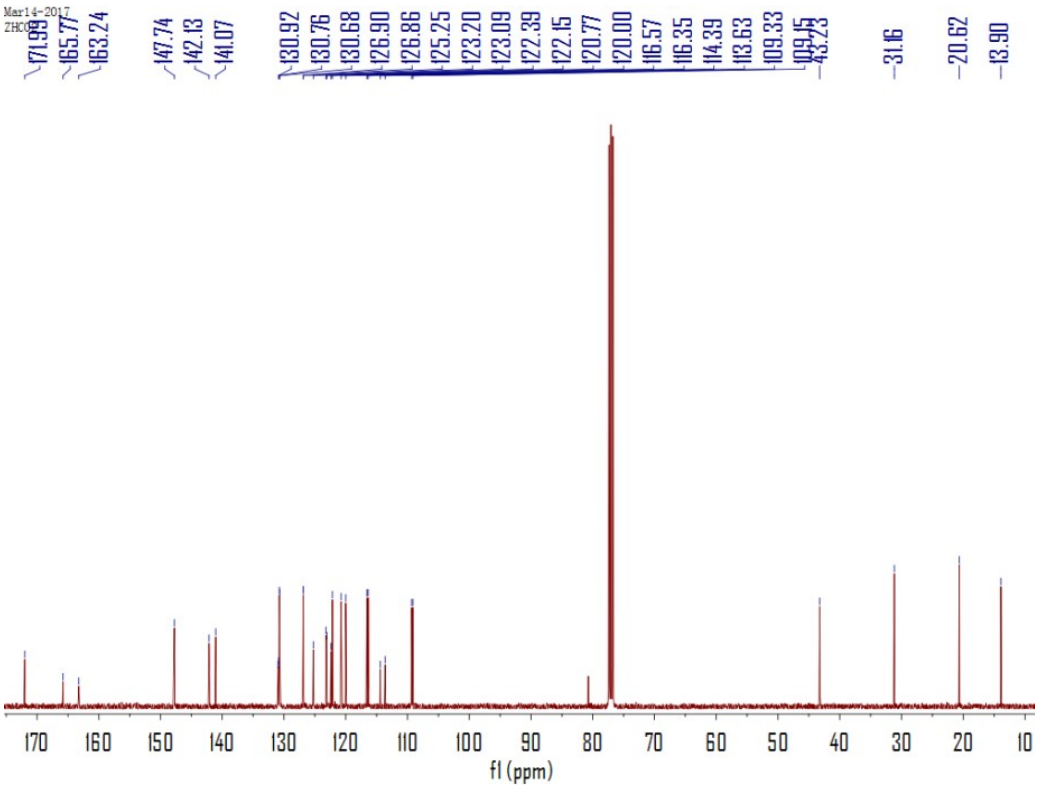

Fig. S3 ^{13}C NMR of compound **3Y** ($CDCl_3$, 400 MHz).

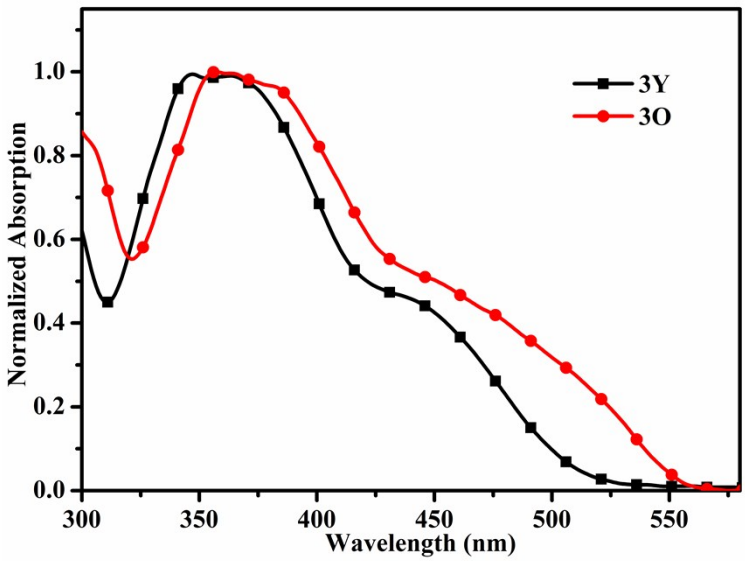

Fig. S4 The absorption spectra for **3Y** and **3O** in the solid state.

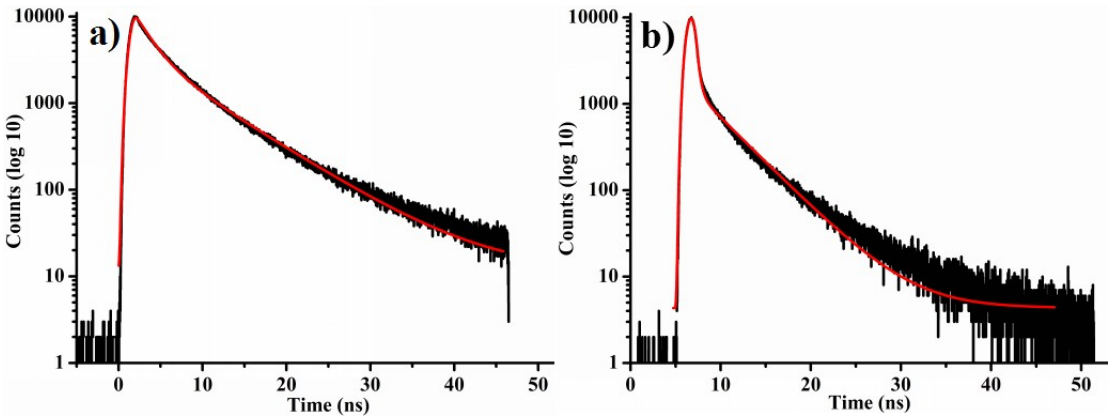

Fig. S5 Lifetime decay curves of **3Y** (a) and **3O** (b).

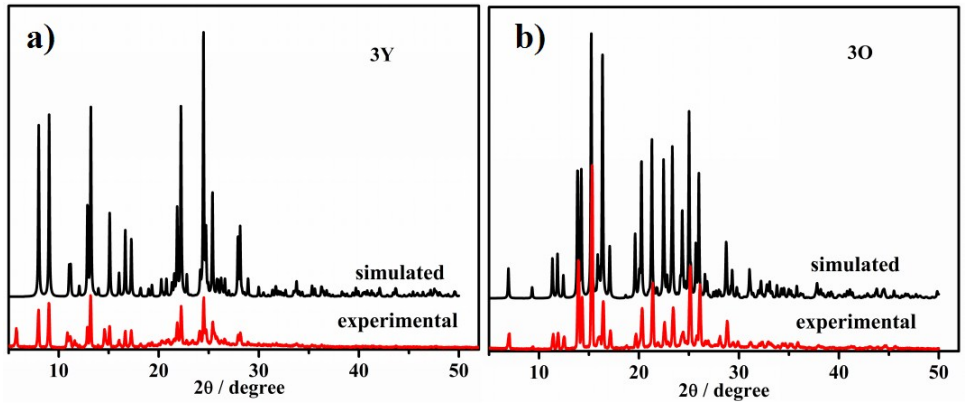

Fig. S6 As-experimental and as-simulated XRD patterns for powder **3Y**, **3O** and crystals **3Y**, **3O**.

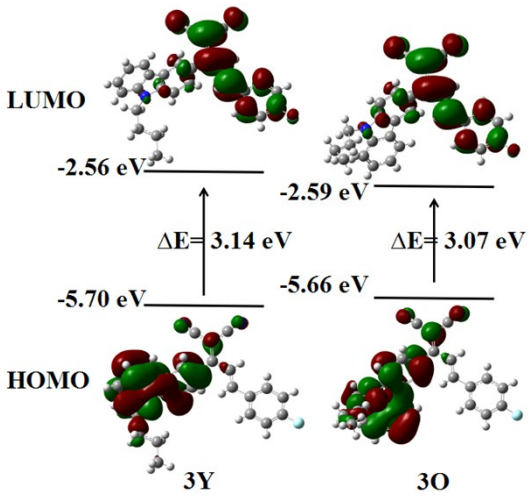

Fig S7 Highest occupied molecular orbital (HOMO), lowest unoccupied molecular orbital (LUMO) diagrams and the energy gap (ΔE) of **3Y** and **3O**

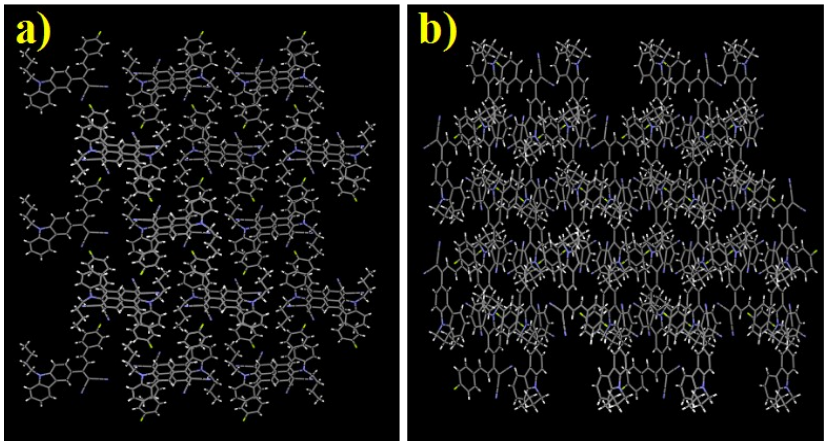

Fig. S8 Molecular stacks in the crystals of **3Y** viewed from the a-axis (a) and c-axis (b).

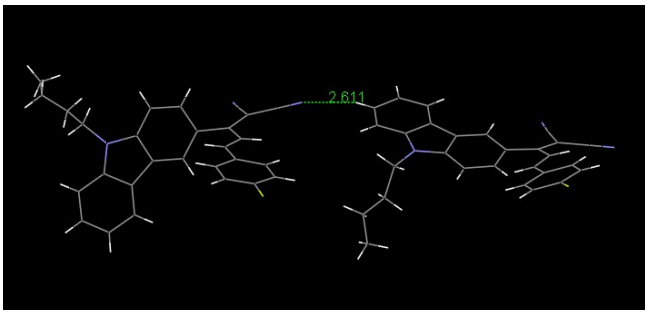

Fig. S9 The molecules of **3O** (structure A and B)

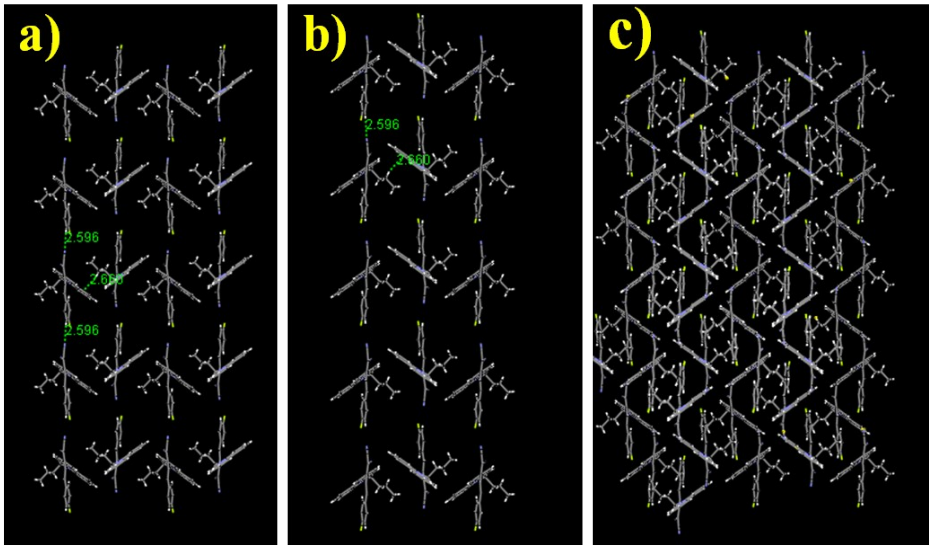

Fig. S10 Molecular stacks in the crystals of **3O**, (a) structure A, (b) structure B, and 3**O** (c) viewed from the a-axis.

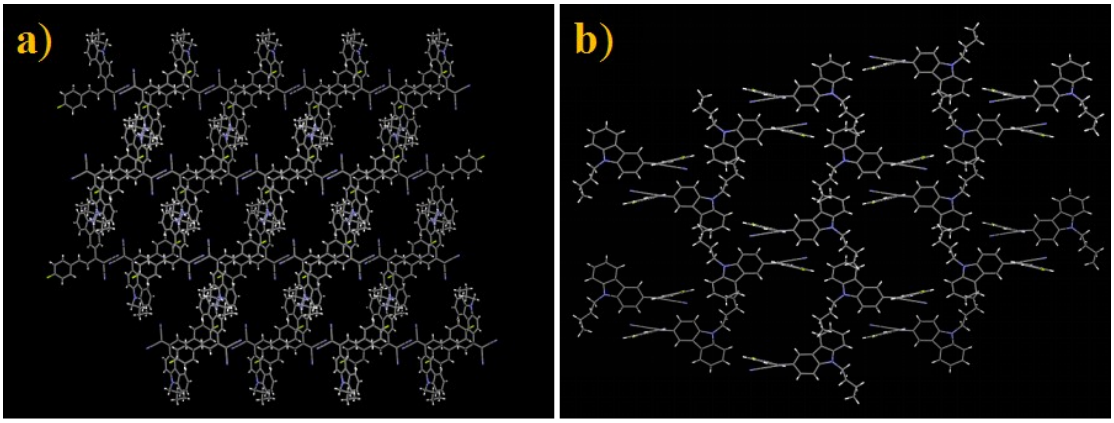

Fig. S11 Molecular stacks in the crystals of **3O** viewed from the b-axis (a) and c-axis (b).

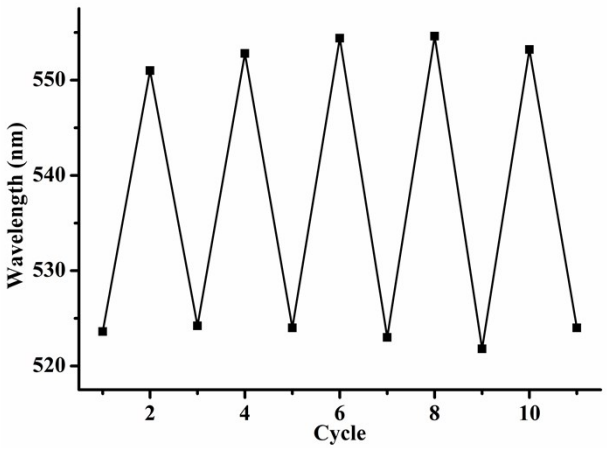

Fig. S12 Cycle behaviors of the maximum emission peaks for **3Y**.

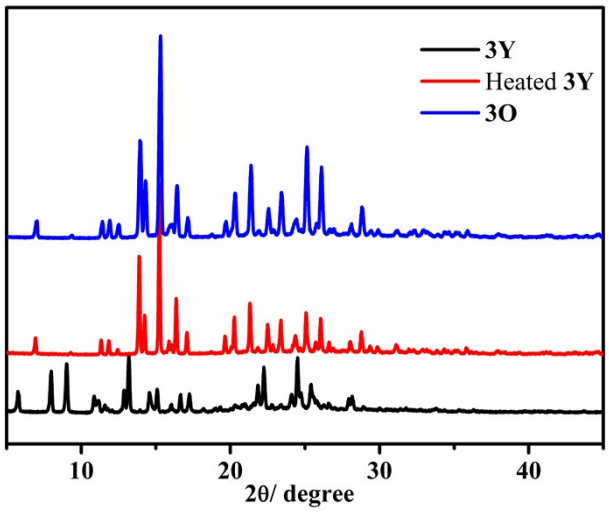

Fig. S13 The PXRD diagram of **3Y**, heated **3Y** and **3O**.